separations

MDPI

*Article*

# Investigation on Li Recovery from Greek Coal Fly Ash Under a Circular Economy Framework: An Experimental Study

**Despina Pentari [1,*], Pagona Makri [1], Panagiotis Xanthopoulos [2] and Despina Vamvuka [1]**

[1] School of Mineral Resources Engineering, Technical University of Crete, 731 00 Chania, Greece
[2] SUNLIGHT Power is Knowledge, Neo Olvio, 672 00 Xanthi, Greece
* Correspondence: dpentari@tuc.gr

## Abstract

Lithium is classified as a critical element and is widely used in a variety of high-tech applications. Within the framework of a circular economy, demand is rising for technologies capable of recovering high-tech metals from waste materials and industrial byproducts. Coal fly ash (CFA) has attracted significant attention as a promising secondary resource for this purpose. Effective recovery requires the assessment of both metal enrichment levels and the underlying binding and leaching characteristics. The present study aims to contribute to advancing lithium recovery technology using coal fly ash as a secondary resource, thereby promoting waste valorization. Fourteen samples of coal fly ash from different power plants were collected and their mineralogy was studied by X-ray powder diffraction (XRD), their major constituents were analyzed by X-ray fluorescence spectroscopy (XRF), and their Li content was determined by inductively coupled plasma mass spectrometry (ICP-MS). Leaching experiments were conducted for selected samples using mineral acids (HCl and HF) and citric acid. Lithium concentrations in the analyzed samples ranged from 80 to 256 mg/kg, indicating enrichment relative to both global ash averages (enrichment factor > 1) and the Earth's crust (enrichment factor > 2). Li in the samples, could be mainly associated with the amorphous fraction present in the samples. Leaching behavior across the samples follows a consistent trend, with hydrofluoric acid exhibiting the highest lithium extraction efficiency—reaching up to 79.9%.

**Keywords:** lithium; coal fly ash; circular economy; secondary resource; leaching experiments

check for updates

Academic Editor: Guoquan Zhang

Received: 17 July 2025
Revised: 29 August 2025
Accepted: 4 September 2025
Published: 15 September 2025

**Citation:** Pentari, D.; Makri, P.; Xanthopoulos, P.; Vamvuka, D. Investigation on Li Recovery from Greek Coal Fly Ash Under a Circular Economy Framework: An Experimental Study. *Separations* **2025**, *12*, 251. https://doi.org/10.3390/separations12090251

## 1. Introduction

Lithium, as a critical element, draws considerable interest from the scientific community due to its diverse applications in advanced technologies. As critical elements are integral to a broad spectrum of modern products, ensuring a stable and sustainable supply has become increasingly important. Though not rare, lithium is identified as critical [1–3], mainly because of the increasing utilization of lithium-ion battery technology. Between 2021 and 2022, the price of battery-grade lithium carbonate ($Li_2CO_3$) surged by 293% [4]. Owing to lithium's distinctive physicochemical properties and its widespread application, global demand is projected to increase fourfold in the coming years [5].

Currently, the world leaders (approximately 90% of global supplies) in lithium production are Chile, Australia, and China with lithium sources being either lithium-rich brines or spodumene and lepidolite minerals [6]. Given lithium's strategic relevance, the recovery of this element from secondary resources is attracting growing attention, particularly within the framework of the circular economy and industrial ecology. Among the proposed secondary materials, spent lithium-ion batteries have received the most extensive research attention [7–9].

It is well known that under certain geological conditions, critical metals can be enriched in coals [6,10,11] with reported concentrations that are comparable, if not greater than those found in traditional ore deposits [12–15]. Accordingly, numerous studies [12,16–24] have identified coal, coal-bearing formations, and coal combustion byproducts as potential alternative sources of lithium, particularly in the context of the transition toward a more sustainable, ”green” economy. Among coal combustion byproducts, fly ash represents 40–90% of the total combustion residue [25,26] and is investigated as a promising Li secondary resource [6,16,25,27–29] with the reported recovery efficiency fluctuating between 42% and 97%. Despite efforts and/or commitments to develop sustainable energy sources, coal continues to play a significant role in electricity generation, contributing approximately 1 billion tons of coal ash each year worldwide [6,21,30], with China producing 500 million tons annually. Coal fly ash is a fine (10–200 µm) powdery combustion residue and is an industrial byproduct that poses significant environmental concerns. The fly ash particles are typically captured from flue gases and collected by appropriate filters. The global utilization/commercialization of fly ash is not uniform. Countries in Europe (Italy and Denmark recycle 100% of the total production), as well as the USA, exhibit high utilization rates, while in other countries like China and South Africa, only 10% of the total production is re-purposed [6,26,30]. The eco-friendly utilization of coal fly ash (CFA) has gained increasing attention across diverse research domains, with numerous strategies proposed to facilitate its recycling and repurposing. These approaches encompass the synthesis of a wide range of value-added products, including construction materials, ceramics, fillers, polymers, zeolites, and fertilizers. Nevertheless, current estimates [6,26] indicate that only approximately 25% of the total fly ash generated is effectively utilized, while the remaining majority is subjected to stockpiling—a practice that poses significant environmental concerns. Consequently, the recovery of critical metals from CFA within the framework of a circular economy has emerged as a focal point of scientific inquiry. This process holds considerable promise, fulfilling a dual objective: advancing waste valorization and contributing to the sustainable management of natural resources.

Recovering critical elements, including lithium, from CFA heavily depends on hydrometallurgy using either direct mineral acid leaching, leaching with more “green” ionic liquids, or deep eutectic solvents, or roasting followed by inorganic leaching. Some researchers have suggested the pre-concentration of critical elements based on physical separation and methods applied to enrich metals in various ores or minerals. In response to the environmental and operational concerns associated with conventional reagents used in these processes, recent studies have proposed the use of certain carboxylic acids as alternative leaching agents. These compounds are readily accessible, less corrosive, and are expected to exert a reduced environmental impact both during and following the leaching procedure [6,26,29,31–34].

The aim of the present study is to investigate the Li content, its enrichment, and its affinity with the matrix in lignite fly ash, in order to contribute to advancing the field of Li recovery technology using coal fly ash as a secondary resource, thus promoting waste valorization. Good knowledge of the mode of occurrence, binding, and leaching characteristics of metals, in addition to their enrichment, is essential for any recovery technique to be efficient. It is within this context that the study demonstrates a considerable degree of novelty, as research focused on lithium recovery from secondary resources other than spent Li-ion batteries remains limited and has only emerged in recent years [6].

## 2. Materials and Methods

In the present study, fourteen fly ash samples were studied. The samples were collected from thermal power plants, which utilize lignite sourced from six regions in Greece, namely Achlada (ACH2006, ACH2008, SKP2024), Ag. Demetrios (AGD2005, AGD2018), Aminteon (AMI2002) and Kardia (KAR2002), Ptolemaida (PTL2008, PTL2024) in northern Greece, and Megalopolis (MEG2008) in Peloponnesus, Greece (Figure 1). The samples were collected on different dates (e.g., AGD2005, AGD2018, PTL2024, PTL2008), and in the case of the PTL2024, samples collected at different hours on the same day (PTL1 2024, PTL2 2024, PTL3 2024, PTL4 2024) were also studied. Samples were chosen based on the previous work of our team [28,29] because they exhibited relatively high Al and Li content, suggesting that they could be considered as Li secondary resources [23,24,31], in addition to possessing different mineralogy. The samples obtained from the respective precipitators were initially air-dried at ambient temperature, followed by oven drying at 105 °C for 24 h, prior to being used for characterization analyses and extraction experiments. The samples underwent no crushing prior to characterization and extraction experiments. All reagents used were of analytical grade. Extraction experiments were conducted in duplicate to ensure the reliability and reproducibility of the results. The measurement variability was minimal, with deviations within ±2%, and all the reported values represent the calculated mean of the replicates.

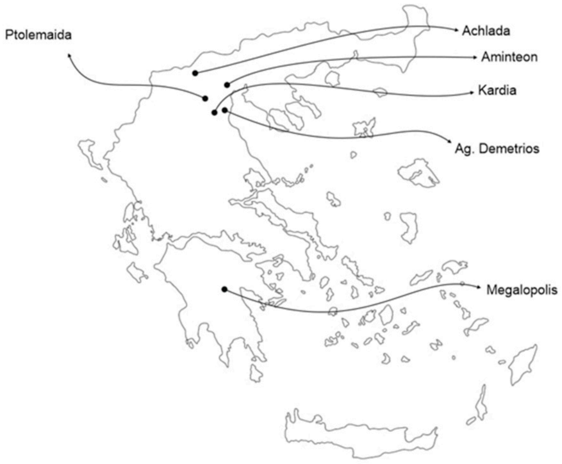

**Figure 1.** Sampling areas.

### *2.1. Sample Characterization*

### 2.1.1. Mineralogical Analysis

Powder X-ray diffraction (XRD) was employed to investigate the mineralogical composition of the samples, utilizing a D8-Advance diffractometer (Bruker AXS, Karlsruhe, Germany) equipped with a Cu X-ray tube, a LynxEye detector, and a Ni-filter. Diffraction patterns were collected over a 2θ range of 2° to 70°, with a step size of 0.02° and a counting time of 0.4 s per step. Corundum was used as an internal standard for semi-quantitative analysis. Qualitative phase identification was performed using Diffracplus EVA (Bruker AXS, Karlsruhe, Germany), while semi-quantitative analysis was carried out using Seifert Autoquan software (Autoquan 2.8).

### 2.1.2. Chemical Analysis and Li Content Determination

The major constituents of the samples (flux beads) were analyzed by X-ray fluorescence spectroscopy (XRF) using the S2 Ranger V5 analyzer by Bruker (city, country), equipped with a Pd anode X-ray tube and a silicon drift detector. Before conducting XRF analysis, the samples were incinerated in a muffle furnace at 950 °C until a constant weight was attained, allowing for the determination of loss on ignition (LOI).

The lithium concentrations in the samples were quantified using inductively coupled plasma mass spectrometry (ICP-MS), following complete dissolution via acid digestion. Specifically, 0.25 g of each sample was treated with an acid mixture (concentrated $HNO_3$, HF, and HCl) in PTFE beakers and heated in a water bath at 80 °C. Upon achieving total dissolution, the resulting solution was diluted to a final volume of 50 mL and stored in a plastic container under refrigeration until ICP-MS analysis. Measurements were performed using the Agilent 7900 ICP-MS system (company, city, country). Lithium concentrations are expressed in mg/kg, calculated based on the initial sample mass (0.25 g) and the final solution volume (50 mL).

### *2.2. Leaching Experiments*

To investigate the leaching behavior of lithium, experiments were conducted on three representative samples: ACH2008, AMI2002, and AGD2018. The selection of ACH2008 and AMI2002 was based on their notably high lithium concentrations, making them suitable candidates for evaluating extraction efficiency. In contrast, AGD2018 was chosen for its distinct mineralogical profile—characterized by a lower proportion of amorphous phases and a higher content of calcite and mica minerals—which allows for comparative analysis of how mineralogical differences influence lithium mobility and leaching dynamics. Hydrochloric acid, hydrofluoric acid, and citric acid were utilized as leaching agents. In a representative experiment—based on prior studies conducted in our laboratory and the relevant literature—0.5 g of fly ash was placed in a PTFE vessel, to which 50 mL of a 2 M acid solution was added. The vessel was sealed and stirred at 600 rpm using a combined hotplate and magnetic stirrer for 2 h at a controlled temperature of 60 °C. Following leaching, the residual ash was separated by filtration using Whatman 42 filter paper. The lithium concentration in the clarified leachate, after acidification with $HNO_3$, was determined via ICP-MS. To assess potential phase transformations induced by the leaching process, the mineralogical composition of the residues was examined. No pH adjustments were made during the procedure; however, both the initial and dynamic pH values were monitored using a pH meter (Inolab Level 1, WTW). In all cases, the pH values ranged between 2.5 and 3.5. The leaching efficiency ($L$) was calculated using the following equation:

$$L = \frac{a * V * 100}{A * m}$$

where $a$ represents the metal concentration in the leachate (mg/L), $V$ denotes the volume of the leaching solution (mL), $A$ corresponds to the metal concentration in the fly ash sample (mg/kg), and $m$ indicates the mass (g) of the sample used in the leaching experiments.

## 3. Results

### *3.1. Sample Characterization*

#### 3.1.1. Mineralogical Analysis

The results (semi-quantitative analysis) of the mineralogy of the samples are illustrated in Table 1 and Figure 2. Amorphous material, represented by a broad peak (amorphous hump) at lower angles ~10°, was the most abundant constituent of all the samples, fluctuating between 25% and 67% (KAR2002 and ACH2008 samples, respectively).

**Table 1.** Mineral and amorphous content in coal ash (% semi-quantitative).

| | MEG 2008 | SKP 2024 | ACH 2006 | ACH 2008 | PTL1 2024 | PTL2 2024 | PTL3 2024 | PTL4 2024 | PTL 2008 | PTL 2000 | AGD 2005 | AGD 2018 | KAR 2002 | AMI 2002 |
|---|---|---|---|---|---|---|---|---|---|---|---|---|---|---|
| **Amorphous** | 53.4 | 43.0 | 60.9 | 67.1 | 29.9 | 31.4 | 27.5 | 30.0 | 36.6 | 37.9 | 40.0 | 44.7 | 34.1 | 48.9 |
| **Anhydrite** $CaSO_4$ | 7.0 | 0.0 | 1.4 | 0.0 | 14.1 | 15.3 | 13.4 | 14.4 | 8.8 | 9.1 | 0.0 | 8.9 | 7.2 | 7.7 |
| **Akermanite** $Ca_2Mg(Si_2O_7)$ | 0.0 | 0.0 | 0.0 | 0.0 | 0.0 | 0.0 | 0.0 | 0.0 | 5.5 | 2.0 | 2.2 | 0.0 | 9.1 | 0.0 |
| **Quartz** $SiO_2$ | 14.8 | 15.9 | 8.9 | 9.0 | 6.8 | 7.9 | 8.6 | 7.6 | 4.5 | 6.7 | 12.3 | 12.3 | 4.3 | 5.6 |
| **Portlandite** $Ca(OH)_2$ | 0.0 | 0.0 | 0.0 | 0.0 | 0.0 | 0.0 | 0.0 | 0.0 | 0.0 | 6.0 | 0.0 | 2.2 | 12.4 | 3.7 |
| **Feldspars** $[(Ca,Na)Al_{1-2}Si_{2-3}O_8-KAlSi_3O_8]$ | 19 | 24.9 | 10 | 9.7 | 10.6 | 13.1 | 15.9 | 13.3 | 9.4 | 9.3 | 12.6 | 4.6 | 5.6 | 16.2 |
| **Calcite** $CaCO_3$ | 2.6 | 4.5 | 2.7 | 0.5 | 3.6 | 3.7 | 4.8 | 6.2 | 21.6 | 5.5 | 3.5 | 11.0 | 9.6 | 4.3 |
| **Brownmillerite** $Ca_2(Al,Fe)_2O_5$ | 0.0 | 0.0 | 0.0 | 0.0 | 7.0 | 4.9 | 6.3 | 7.6 | 7.3 | 11.1 | 0.0 | 0.0 | 11.9 | 5.3 |
| **Gehlenite** $Ca_2Al[AlSiO_7]$ | 0.0 | 0.0 | 0.0 | 0.0 | 14.7 | 19.6 | 13.4 | 13.9 | 6.5 | 12.4 | 5.5 | 2.6 | 0.0 | 0.0 |
| **Dolomite** $CaMg(CO_3)_2$ | 0.0 | 1.1 | 0.0 | 0.0 | 0.0 | 0.0 | 0.0 | 0.0 | 0.0 | 0.0 | 0.0 | 0.0 | 0.0 | 0.0 |
| **Mica** $[KAl_2(AlSi_3O_{10})(F,OH)_2]$ | 0.0 | 4.0 | 0.0 | 0.0 | 4.4 | 1.7 | 3.6 | 0.0 | 0.0 | 0.0 | 0.0 | 4.0 | 2.5 | 1.7 |
| **Dicalcium silicate** $Ca_2SiO_4$ | 0.0 | 0.0 | 0.0 | 0.0 | 0.0 | 0.0 | 0.0 | 0.0 | 0.0 | 0.0 | 0.0 | 0.0 | 0.0 | 5.0 |
| **Calcium oxide** $CaO$ | 0.0 | 0.0 | 0.0 | 0.0 | 5.7 | 0.0 | 5.5 | 7.1 | 0.0 | 0.0 | 0.0 | 6.9 | 2.4 | 1.6 |
| **Hematite** $Fe_2O_3$ | 3.3 | 0.0 | 1.7 | 1.6 | 2.3 | 2.5 | 1.0 | 0.0 | 0.0 | 0.0 | 1.0 | 1.6 | 0.0 | 0.0 |
| **Mullite** $Al_6Si_2O_{13}$ | 0.0 | 0.0 | 12.0 | 12.1 | 0.0 | 0.0 | 0.0 | 0.0 | 0.0 | 0.0 | 0.0 | 0.0 | 0.0 | 0.0 |
| **Spinel** $MgAl_2O_4$ | 0.0 | 0.0 | 2.4 | 0.0 | 0.0 | 0.0 | 0.0 | 0.0 | 0.0 | 0.0 | 0.0 | 0.0 | 0.0 | 0.0 |
| **Diopside** $MgCaSi_2O_6$ | 0.0 | 0.0 | 0.0 | 0.0 | 0.0 | 0.0 | 0.0 | 0.0 | 0.0 | 0.0 | 5.1 | 0.0 | 0.0 | 0.0 |
| **Periclase** $MgO$ | 0.0 | 0.0 | 0.0 | 0.0 | 0.9 | 0.0 | 0.0 | 0.0 | 0.0 | 0.0 | 1.2 | 0.8 | 0.0 | 0.0 |
| **Geothite** a-FeO(OH) | 0.0 | 0.0 | 0.0 | 0.0 | 0.0 | 0.0 | 0.0 | 0.0 | 0.0 | 0.0 | 0.0 | 0.3 | 0.0 | 0.0 |

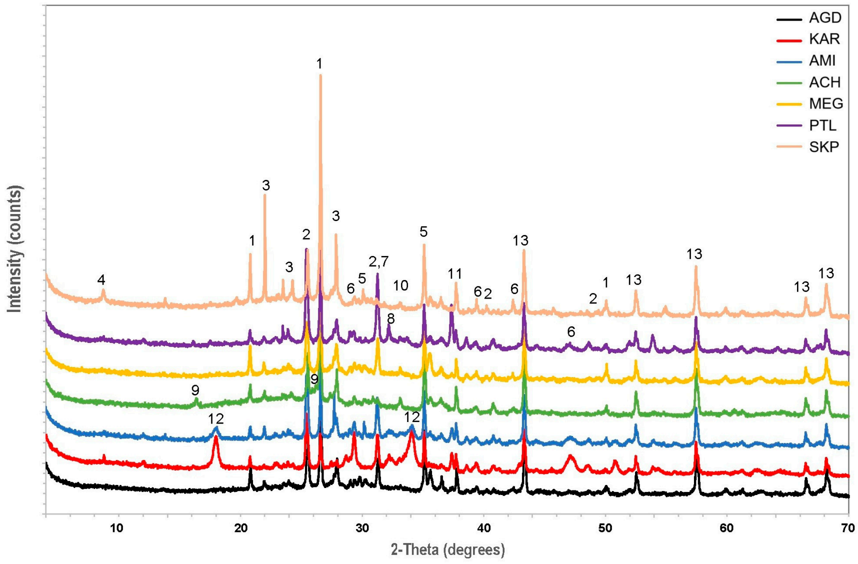

**Figure 2.** X-ray diffraction (XRD) patterns for seven representative samples of the regions studied. 1: Quartz, 2: Anhydrite, 3: Feldspar, 4: Mica, 5: Pyroxene, 6: Calcite, 7: Gehlenite, 8: Dicalcium Silicate, 9: Mullite, 10: Hematite, 11: Lime, 12: Portlandite, 13: Corundum.

This result is in accordance with the data in the literature [22,23,28,29,34–37], where fly ash is reported to contain significant amounts of amorphous glassy material. The samples possess different mineralogy, with the main mineral phases that are encountered being calcite (22% and 12% in the case of PTL2008 and KAR2002), feldspars (19% and 15% for the samples SKP2024 and MGP2008, respectively), and mullite (12% for both ACH2008 samples). The samples collected at different hours on the same day showed no significant mineralogical differences, while the samples collected from different thermal power plants, which utilize lignite sourced from the same region, exhibited different mineralogy, which could be attributed to the combustion conditions of the plants. Although no lithium-bearing minerals were detected, it is noteworthy that mullite—a mineral characteristic of high-alumina fly ash and potentially linked to elevated lithium concentrations—was observed exclusively in the ACH2008 samples [20,38–40]. Additionally, samples SKP2024 and PTL1 2024 contained minor amounts of mica (<4.5%), which may include lithium-bearing phases such as muscovite. These findings suggest that the Li encountered in the samples studied is mainly associated with amorphous material, and this is in accordance with other research findings [20,28,29,38,39].

### 3.1.2. Chemical Analysis and Li Content

The major element composition, presented in Table 2 as the weight percent (wt%) of metal oxides, aligns well with the corresponding mineralogical data. Silicon and calcium were identified as the predominant constituents in the AGD samples, whereas silicon and aluminum dominated the ACH samples. Based on their low CaO content and elevated aluminosilicate levels, the ACH, SKP, MGP, and AGD2005 samples are categorized as Class F fly ash. In contrast, the remaining samples, characterized by relatively high calcium content, are classified as Class C [41]. The loss on ignition of the samples, which is also reported in Table 2, fluctuated from 0.61% to 15% (ACH2008 and SKP2024, respectively). The fluctuation could be explained by the mineralogy of the samples but could also be attributed to the unburned carbon encountered in the samples, depending on the combustion process and combustion efficiency of the different thermal plants. The Li content of the samples is illustrated in Figure 3.

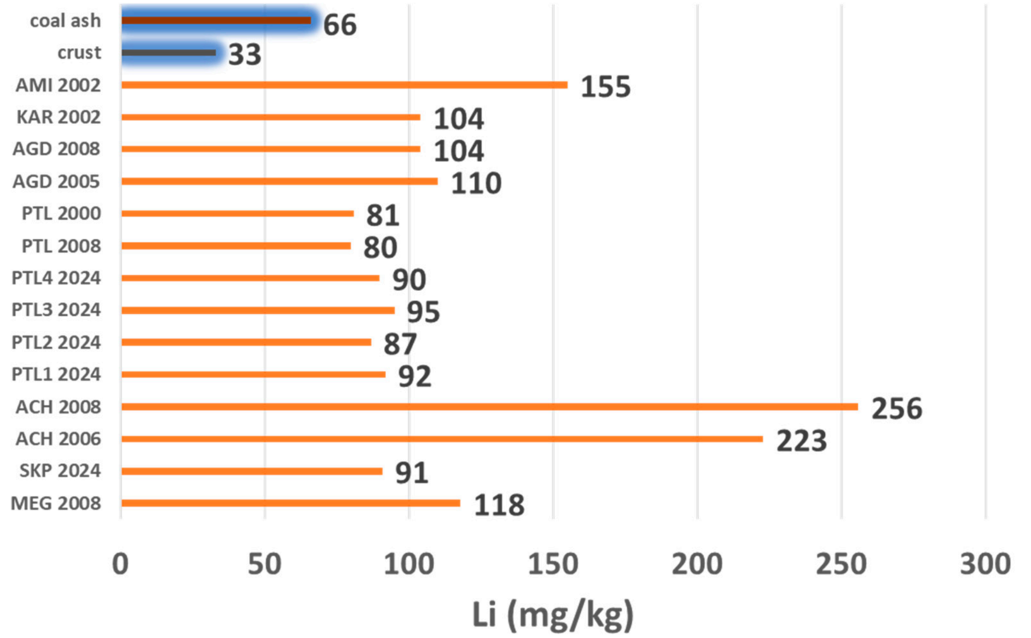

**Figure 3.** Li contents (mg/kg) of the studied fly ash samples compared to fly ash globally, and earth crust.

**Table 2.** The major elements (as oxides %) and corresponding loss on ignition (LOI) for the studied fly ash samples.

| | $Na_2O$ (%) | MgO (%) | $K_2O$ (%) | CaO (%) | $TiO_2$ (%) | $Al_2O_3$ (%) | $SiO_2$ (%) | $P_2O_5$ (%) | $Cr_2O_3$ (%) | MnO (%) | $Fe_2O_3$ (%) | ZnO (%) | $SO_3$ (%) | BaO (%) | SrO (%) | LOI | TOTAL |
|---|---|---|---|---|---|---|---|---|---|---|---|---|---|---|---|---|---|
| **MEG 2008** | 0.7 | 3.4 | 1.6 | 14.4 | 0.5 | 19.2 | 44.5 | 0.3 | 0.0 | 0.1 | 9.5 | 0.0 | 1.8 | 0.3 | 0.1 | 3.7 | 100 |
| **SKP 2024** | 0.8 | 3.2 | 1.9 | 3.4 | 0.5 | 19.2 | 49.2 | 0.0 | 0.0 | 0.1 | 6.1 | 0.0 | 0.3 | 0.3 | 0.0 | 15.1 | 100 |
| **ACH 2006** | 1.0 | 4.0 | 2.6 | 4.3 | 0.6 | 26.4 | 51.1 | 0.2 | 0.0 | 0.1 | 7.9 | 0.0 | 0.3 | 0.3 | 0.0 | 2.0 | 100 |
| **ACH 2008** | 0.9 | 3.9 | 2.6 | 4.3 | 0.6 | 27.3 | 51.5 | 0.1 | 0.0 | 0.1 | 7.9 | 0.0 | 0.3 | 0.4 | 0.0 | 0.6 | 100 |
| **PTL1 2024** | 0.8 | 4.4 | 1.0 | 33.2 | 0.6 | 17.4 | 27.5 | 0.5 | 0.0 | 0.0 | 5.7 | 0.0 | 5.4 | 0.3 | 0.0 | 3.1 | 100 |
| **PTL2 2024** | 0.7 | 4.3 | 1.0 | 30.9 | 0.6 | 18.0 | 30.3 | 0.2 | 0.0 | 0.0 | 5.5 | 0.0 | 5.5 | 0.4 | 0.0 | 2.9 | 100 |
| **PTL3 2024** | 1.1 | 4.9 | 1.0 | 33.5 | 0.6 | 16.3 | 28.1 | 0.4 | 0.0 | 0.0 | 5.5 | 0.0 | 5.2 | 0.3 | 0.0 | 3.0 | 100 |
| **PTL4 2024** | 1.1 | 4.4 | 1.0 | 32.1 | 0.5 | 15.6 | 30.0 | 0.4 | 0.0 | 0.0 | 5.9 | 0.0 | 5.2 | 0.1 | 0.0 | 4.1 | 100 |
| **PTL 2008** | 0.8 | 4.3 | 0.8 | 31.0 | 0.6 | 14.6 | 26.3 | 0.3 | 0.0 | 0.0 | 4.9 | 0.0 | 4.1 | 0.3 | 0.0 | 11.9 | 100 |
| **PTL 2000** | 0.7 | 4.3 | 1.0 | 32.6 | 0.6 | 16.8 | 25.7 | 0.4 | 0.0 | 0.0 | 5.5 | 0.0 | 5.1 | 0.3 | 0.0 | 6.9 | 100 |
| **AGD 2005** | 0.9 | 3.7 | 1.6 | 15.5 | 0.4 | 20.0 | 45.0 | 0.3 | 0.0 | 0.1 | 8.9 | 0.0 | 1.5 | 0.5 | 0.1 | 1.8 | 100 |
| **AGD 2018** | 1.0 | 4.4 | 0.9 | 28.7 | 0.5 | 16.5 | 32.4 | 0.4 | 0.1 | 0.0 | 4.1 | 0.0 | 3.8 | 0.3 | 0.0 | 6.7 | 100 |
| **KAR 2002** | 1.1 | 4.5 | 0.8 | 38.4 | 0.4 | 16.2 | 20.2 | 0.2 | 0.0 | 0.1 | 5.3 | 0.0 | 3.8 | 0.2 | 0.0 | 9.8 | 100 |
| **AMI 2002** | 0.7 | 4.1 | 1.1 | 26.5 | 0.5 | 16.2 | 36.7 | 0.4 | 0.0 | 0.1 | 5.7 | 0.0 | 3.2 | 0.4 | 0.0 | 5.0 | 100 |

Among the analyzed fly ash samples, ACH2008 exhibited the highest lithium concentration at 256 mg/kg, followed by ACH2006 with 223 mg/kg, while PTL2008 showed the lowest value at 80 mg/kg. These findings are consistent with previously reported data [16,24,28,29,40]. For context, the average lithium concentration in the Earth's crust is 33 mg/kg, and coal ash globally is reported to contain 66 mg/kg [41,42]. Accordingly, all the studied samples demonstrated lithium enrichment, with enrichment factors exceeding 1 relative to global coal ash and greater than 2 compared to crustal abundance. Notably, the lithium content in ACH2008 (256 mg/kg or 0.06 wt% $Li_2O$) is comparable to concentrations found in industrial-grade lithium-bearing pegmatite deposits in China [16].

To study the correlation between the measured Li and the major element content, as well as the minerals identified, linear correlation coefficients were utilized. As depicted in Figure 4, Li showed a strong positive correlation ($R^2 > 0.75$) with aluminum and amorphous material.

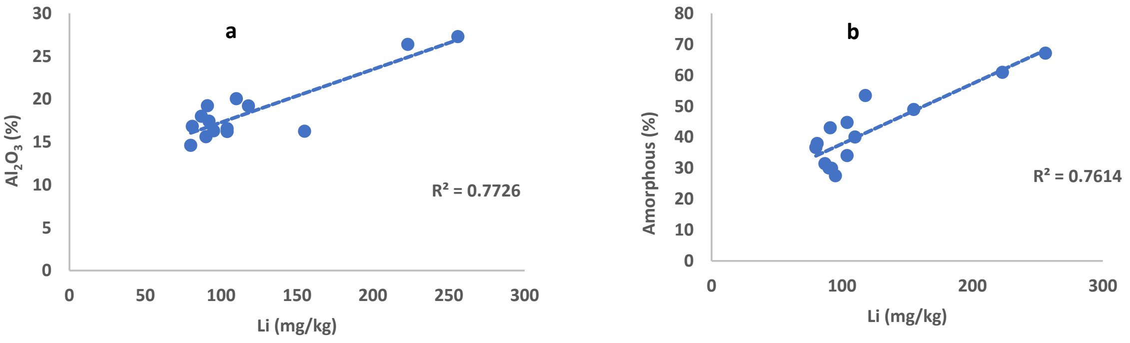

**Figure 4.** Li correlation with (**a**) Al content and (**b**) with amorphous material.

### 3.2. Leaching Experiments

The results of the leaching experiments are illustrated in Figure 5, where the leaching efficiency (L) for the three leaching agents is illustrated.

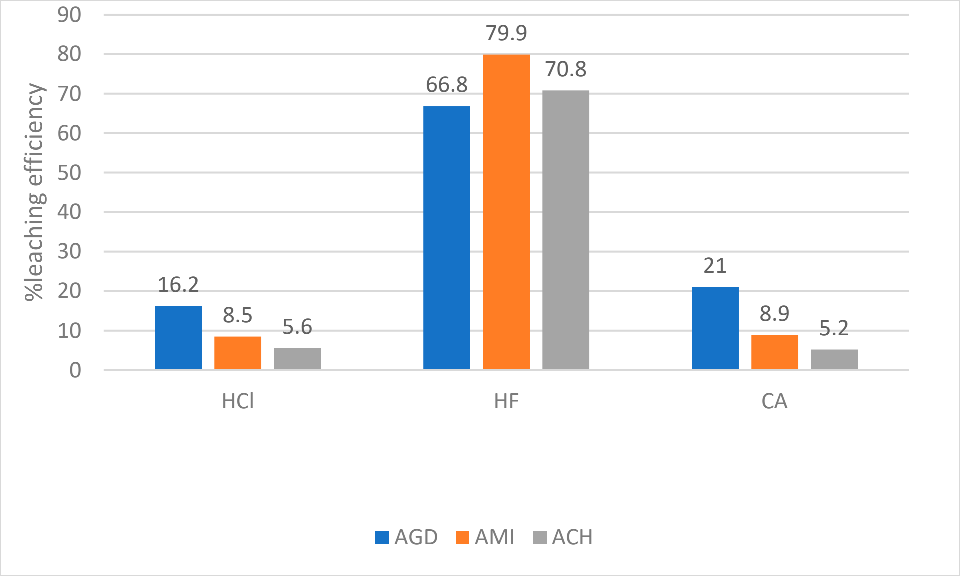

**Figure 5.** The leaching efficiency. Experimental conditions: solid to liquid ratio: 0.5 g/50 mL, temperature: 60 °C, time: 2 h, acid concentration: 2 M.

Hydrofluoric acid appears to be the most efficient leaching agent for the three studied fly ash samples, with the highest observed leaching efficiency being 79.9% for the AMI2002 sample. Hydrochloric and citric acids exhibit far lower leaching efficiencies up to 21% in the case of the AGD2018 sample when citric acid was used as the leaching agent, whereas for the ACH2008 sample, low leaching efficiencies are observed. The observed leaching behavior is in accordance with the literature [6,28,29,32,33] and could be attributed to the type and corresponding stability constant values of complexes or precipitates that are expected to form in the specific leaching conditions. The relatively high leaching efficiency of HF 2 M, which is expected [22,26,43] to selectively attack glassy material, supports the hypothesis that the lithium in the samples is mainly associated with the amorphous material. While hydrofluoric acid (HF) demonstrated the highest lithium extraction efficiency, its use raises significant environmental and safety concerns; therefore, a critical assessment of its sustainability and practicality for large-scale industrial applications is needed, taking into account regulatory constraints, waste management requirements, and potential alternatives that offer lower ecological and operational risks. With the aim of attaining a better insight into the complex chemical transformations that take place throughout the leaching, work is in progress to study the effect of the liquid-to-solid ratio, leaching duration, temperature, and acid concentration on the process, as well as the morphology of the experiment's residues.

Mineralogical analysis of the leaching residues, as depicted in Figure 6 through representative examples from the AGD2018 and AMI2002 samples, revealed that calcite and mica were the main mineral phases attacked by the acids employed as leaching agents. This observation leads to the hypothesis that the mica identified in the AGD2018 and AMI2002 samples may contain Li-bearing micas susceptible to chemical dissolution during leaching.

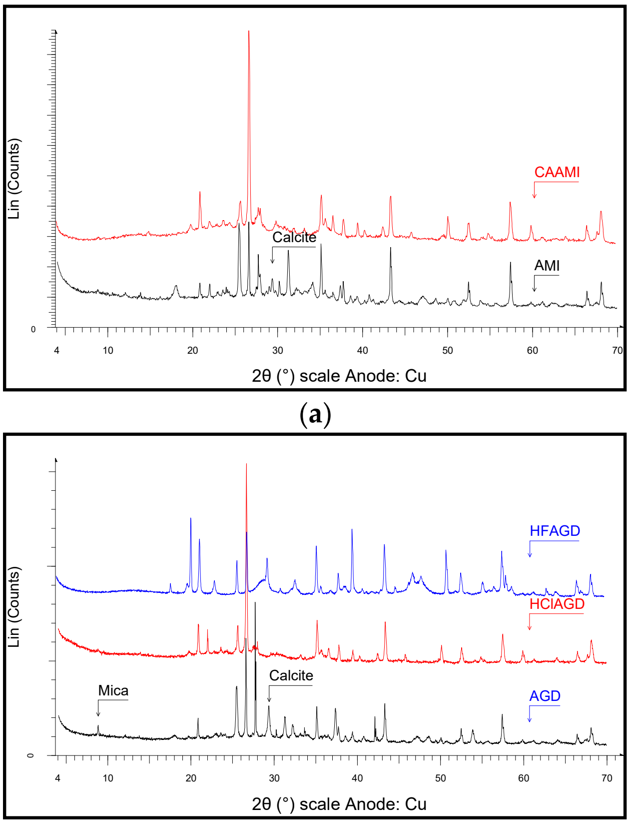

(**a**)

(**b**)

**Figure 6.** Mineralogy of AMI2002 (**a**) and AGD2018 (**b**) compared to the mineralogy of residues after leaching with citric acid (CAAMI), hydrochloric acid (HClAGD), and hydrofluoric acid (HFAGD).

## 4. Conclusions

The lithium content of the samples, which fluctuates between 80 and 256 mg/kg, could be considered enriched (enrichment factor > 1 compared to ash worldwide and >2 compared to the Earth's crust). The relatively high Li content (256 mg/kg Li or 0.06 wt% $Li_2O$) encountered in the ACH fly ash is comparable to industrial-grade Li-bearing pegmatite deposits. Moreover, factors such as the year of sampling and the combustion conditions across different power plants significantly influence the mineralogical composition and loss on ignition of the samples. A strong positive correlation between the Li content and amorphous material, along with the absence of detectable Li-bearing phases in high-Li samples, suggests that lithium is primarily hosted within the amorphous glassy matrix. This interpretation is further supported by the leaching experiments and the mineralogical analyses of the resulting residues. Micas identified in the AGD and AMI samples may contain Li-bearing phases that are susceptible to attack by the leaching agents applied. Leaching behavior across the samples followed a consistent trend, with hydrofluoric acid exhibiting the highest lithium extraction efficiency—reaching up to 79.9% in the AMI sample. Laboratory-scale evidence highlights the potential for lithium recovery from the studied CFA samples, particularly when using HF as a leaching agent. However, to assess the practical and industrial feasibility of this approach, further studies are required, including larger-scale testing and comprehensive evaluations of cost, safety, and environmental impact. Continued research employing alternative leaching agents—such as NaOH to target amorphous materials or mixtures of carboxylic acids—and investigation into the effects of the liquid-to-solid ratio, leaching duration, temperature, and acid concentration on the leaching process will provide deeper insight into lithium binding and leaching behavior. These efforts will contribute to the development of efficient and sustainable lithium recovery procedures.

**Author Contributions:** Conceptualization, D.P.; methodology, D.P.; software, D.P. and P.M.; validation, D.P. and D.V.; formal analysis, D.P. and P.M.; investigation, P.X. and D.P.; resources, D.P. and P.X.; data curation, D.P. and P.M.; writing—original draft preparation, D.P.; writing—review and editing, D.P. and D.V.; visualization, D.P. and P.M.; supervision, D.P.; project administration, D.P. All authors have read and agreed to the published version of the manuscript.

**Funding:** This research was funded by “SUNLIGHT power is knowledge”.

**Data Availability Statement:** The original contributions presented in this study are included in the article. Further inquiries can be directed to the corresponding author.

**Conflicts of Interest:** Author Panagiotis Xanthopoulos was employed by the company “SUNLIGHT power is knowledge”. The remaining authors declare that the research was conducted in the absence of any commercial or financial relationships that could be construed as a potential conflict of interest. The authors declare that this study received funding from “SUNLIGHT power is knowledge”. The funder was not involved in the study design, collection, analysis, interpretation of data, the writing of this article or the decision to submit it for publication.

## References

1. Regulation (EU) 2024/1252 of the European Parliament and of the Council of 11 April 2024 Establishing a Framework for Ensuring a Secure and Sustainable Supply of Critical Raw Materials and Amending Regulations (EU) No 168/2013, (EU) 2018/858, (EU) 2018/1724 and (EU) 2019/1020 Text with EEA Relevance. Available online: https://eur-lex.europa.eu/eli/reg/2024/1252/oj (accessed on 2 March 2024).
2. Bradley, D.C.; Stillings, L.L.; Jaskula, B.W.; Munk, L.A.; McCauley, A.D. Lithium. In *Critical Mineral Resources of the United States—Economic and Environmental Geology and Prospects for Future Supply*; Schulz, K.J., De Young, J.H., Jr., Seal, R.R., II, Bradley, D.C., Eds.; U.S. Geological Survey: Reston, VA, USA, 2017; pp. K1–K21. Available online: https://pubs.usgs.gov/publication/pp1802K (accessed on 2 March 2024).
3. Garside, M. Average Lithium Carbonate Price from 2010 to 2021. Statista. 7 March 2022. Available online: https://www.statista.com/statistics/606350/batterygrade-lithium-carbonate-price/ (accessed on 27 November 2023).
4. U.S. Geological Survey. Available online: https://www.usgs.gov/news/national-news-release/us-geological-survey-releases-2022-list-critical-minerals (accessed on 2 March 2024).
5. Rudnik, E. Coal and Coal By-Products as Unconventional Lithium Sources: A Review of Occurrence Modes and Hydrometallurgical Strategies for Metal Recovery. *Minerals* **2024**, *14*, 849. [CrossRef]
6. Liu, C.; Lin, J.; Cao, H.; Zhang, Y.; Sun, Z. Recycling of spent lithium-ion batteries in view of lithium recovery: A review. *J. Clean. Prod.* **2019**, *228*, 801–813. [CrossRef]
7. Ratuela, R.; Yadav, B.R.; Kumar, S. A review on technologies for recovery of metals from waste lithium-ion batteries. *J. Power Sourc.* **2023**, *580*, 233248.
8. Cheng, Q.; Wang, Z.; Wang, Y.; Li, J.T.; Fu, H. Recent advances in preferentially selective Li recovery from spent lithium-ion batteries: A review. *J. Environ. Chem. Eng.* **2024**, *12*, 112903. [CrossRef]
9. Sun, Y.Z.; Zhao, C.L.; Li, Y.H.; Wang, J.X.; Lin, M.Y. Li distribution and mode of occurrences in Li-bearing coal seam 9 from Pingshuo Mining District, Ningwu Coalfield, northern China. *Energy Educ. Sci. Technol. Part A Energy Sci. Res.* **2013**, *31*, 27–38.
10. Seredin, V.V.; Dai, S.; Sun, Y.; Chekryzhov, I.Y. Coal deposits as a promising source of rare metals for alternative power and energy-efficient technologies. *Appl. Geochem.* **2013**, *31*, 1–11. [CrossRef]
11. Dai, S.; Finkelman, R.B. Coal as a promising source of critical elements: Progress and future prospects. *Int. J. Coal Geol.* **2018**, *186*, 155–164. [CrossRef]
12. Talan, D.; Huang, Q.; Liang, L.; Song, X. Conceptual Process Development for Recovery of Thorium, Uranium, and Rare Earths from Coarse Coal Refuse. *Miner. Process. Extr. Metall. Rev.* **2022**, *44*, 330–345. [CrossRef]
13. Bhatt, A.; Priyadarshini, S.; Mohanakrishnan, A.A.; Abri, A.; Sattler, M.; Techapaphawit, S. Physical, chemical, and geotechnical properties of coal fly ash: A global review. *Case Stud. Constr. Mater.* **2019**, *11*, e00263. [CrossRef]
14. Dai, S.; Yan, X.; Ward, C.R.; Hower, J.C.; Zhao, L.; Wang, X.; Finkelman, R.B. Valuable elements in Chinese coals: A review. *Int. Geol. Rev.* **2018**, *60*, 590–620. [CrossRef]
15. Finkelman, R.B.; Dai, S.F.; French, D. The importance of minerals in coal as the hosts of chemical elements: A review. *Int. J. Coal Geol.* **2019**, *212*, 103251. [CrossRef]

16. Hagelüken, C.; Goldmann, D. Recycling and circular economy—Towards a closed loop for metals in emerging clean technologies. *Miner. Econ.* **2022**, *35*, 539–562. [CrossRef]
17. Hu, P.; Hou, X.; Zhang, J.; Li, S.; Wu, H.; Damo, A.; Xi, X. Distribution and Occurrence of Lithium in High-Alumina-Coal Fly Ash. *Int. J. Coal Geol.* **2018**, *189*, 27–34. [CrossRef]
18. Marinakis, V.; Flamos, A.; Stamtsis, G.; Georgizas, I.; Maniatis, Y.; Doukas, H. The efforts towards and challenges of Greece's post-lignite era: The case of megalopolis. *Sustainability* **2020**, *12*, 10575. [CrossRef]
19. Qin, S.; Zhao, C.; Li, Y.; Zhang, Y. Review of coal as a promising source of lithium. *Int. J. Oil Gas Coal Technol.* **2015**, *9*, 215–229. [CrossRef]
20. Sahoo, P.K.; Kim, K.; Powell, M.A.; Equeenuddin, S.M. Recovery of metals and other beneficial products from coal fly ash: A sustainable approach for fly ash management. *Int. J. Coal Sci. Technol.* **2016**, *3*, 267–283. [CrossRef]
21. Talan, D.; Huang, Q. A review study of rare Earth, Cobalt, Lithium, and Manganese in Coal-based sources and process development for their recovery. *Miner. Eng.* **2022**, *189*, 107897. [CrossRef]
22. Zhang, W.; Honaker, R. Characterization and recovery of rare earth elements and other critical metals (Co, Cr, Li, Mn, Sr, and V) from the calcination products of a coal refuse sample. *Fuel* **2020**, *267*, 117236. [CrossRef]
23. Zou, J.; Cheng, L.; Guo, Y.; Wang, Z.; Tian, H.; Li, T. Mineralogical and geochemical characteristics of lithium and rare earth elements in high-sulfur coal from the donggou mine, Chongqing, southwestern China. *Minerals* **2020**, *10*, 627. [CrossRef]
24. Zhou, M.; Zhao, L.; Wang, X.; Nechaev, V.; French, D.; Spiro, B.; Dai, S. Mineralogy and Geochemistry of the Late Triassic Coal from the Caotang Mine, Northeastern's Sichuan Basin, China, with Emphasis on the Enrichment of the Critical Element Lithium. *Ore Geol. Rev.* **2021**, *139*, 104582. [CrossRef]
25. Zhao, L.; Dai, S.; Nechaev, V.; Nechaeva, E.; Graham, I.; French, D. Enrichment Origin of Critical Elements (Li and Rare Earth Elements) and A Mo-U-Se-Re Assemblage in Pennsylvanian Anthracite from the Jincheng Coalfield, Southeastern Qinshui Basin, Northern China. *Ore Geol. Rev.* **2019**, *115*, 103184. [CrossRef]
26. Nsiah-gyambibi, R.; Sokama-Neuyam, Y.A.; Bokakye, P.; Ampomah, W.; Aggrey, W.N.; Wang, S. Valorization of coal fly ash (CFA): A multi-industry review. *Int. J. Environ. Sci. Technol.* **2023**, *20*, 12807–12822. [CrossRef]
27. Baig, S.Y.; Yousaf, M. Coal fired power plants: Emission problems and controlling techniques. *J. Earth Sci. Clim. Change* **2017**, *8*, 104. [CrossRef]
28. Pentari, D.; Vlachaki, E.; Fazaki, M.E.; Stratakis, A. Lithium in Greek coal fly ashes: Contents and characterization by sequential extraction. *Sustainability* **2024**, *16*, 1442. [CrossRef]
29. Pentari, D.; Varouchakis, E.; Cheiladaki, I.; Keravnopoulou, D.; Partsalaki, E. Carboxylic acid-assisted leaching of critical elements from coal fly ash: Experimental and simulation studies. *Glob. Nest J.* **2024**, *26*, 06013. [CrossRef]
30. Rezaei, H.; Shafaei, S.Z.; Abdollahi, H.; Shahidi, A.; Ghassa, S. A sustainable method for germanium, vanadium and lithium extraction from coal fly ash: Sodium salts roasting and organic acids leaching. *Fuel* **2022**, *312*, 122844. [CrossRef]
31. Vilakazi, A.Q.; Ndlovu, S.; Chipise, L.; Shemi, A. The Recycling of Coal Fly Ash: A Review on Sustainable Developments and Economic Considerations. *Sustainability* **2022**, *14*, 1958. [CrossRef]
32. Manurung, H.; Rosita, W.; Anggara, F.; Petrus, H.B.T.M.; Bendiyasa, I.M. Leaching of REY from non-magnetic coal fly ash with acetic acid. *IOP Conf. Ser. Mater. Sci. Eng.* **2020**, *778*, 012005. [CrossRef]
33. Prihutami, P.; Prasetya, A.; Sediawan, W.B.; Petrus, H.T.; Anggara, F.Y. Study on Rare Earth Elements Leaching from Magnetic Coal Fly Ash by Citric Acid. *J. Sustain. Metall.* **2021**, *7*, 1241–1253. [CrossRef]
34. Prihutami, P.; Sediawan, W.B.; Astuti, W.; Prasetya, A. Effect of temperature on rare earth elements recovery from coal fly ash using citric acid. *IOP Conf. Ser. Mater. Sci. Eng.* **2020**, *742*, 012040. [CrossRef]
35. Aughenbaugh, K.L.; Stutzman, P.; Juenger, M.C.G. Identifying glass compositions in fly ash. *Front. Mater.* **2016**, *3*, 1. [CrossRef]
36. Adamidou, K.; Kassoli-Fournaraki, A.; Filippidis, A.; Christanis, K.; Amanatidou, E.; Tsikritzis, L.; Patrikaki, O. Chemical investigation of lignite samples and their ashing products from Kardia lignite field of Ptolemais, Northern Greece. *Int. J. Coal Geol.* **2007**, *86*, 2502–2508. [CrossRef]
37. Filippidis, A.; Georgakopoulos, A. Mineralogical and chemical investigation of fly ash from the Main and Northern lignite fields in Ptolemais. *Int. J. Coal Geol.* **1992**, *71*, 373–376. [CrossRef]
38. Koukouzas, N.; Kalaitzidis, S.P.; Ward, C.R. Organic petrographical, mineralogical and geochemical features of the Achlada and Mavropigi lignite deposits. NW Macedonia, Greece. *Int. J. Coal Geol.* **2010**, *83*, 387–395. [CrossRef]
39. Ward, C. Analysis, Origin and Significance of Mineral Matter in Coal: An Updated Review. *Int. J. Coal Geol.* **2016**, *165*, 1–27. [CrossRef]
40. Gomes, S.; François, M. Characterization of mullite in silicoaluminous fly ash by XRD, TEM, and 29Si MAS NMR. *Cem. Concr. Res.* **2000**, *30*, 175–181. [CrossRef]
41. Finkelman, R. Trace and Minor Elements in Coal. In *Organic Chemistry*; Engel, I.M., Macko, S., Eds.; Plenum: New York, NY, USA, 1993; pp. 693–1607. [CrossRef]

42. Ketris, Y.E.; Yudovich, Y. Estimations of Clarkes for Carbonaceous biolithes: World averages for trace element contents in black shales and coals. *Int. J. Coal Geol.* **2009**, *78*, 135–148. [CrossRef]
43. Xu, F.; Qin, S.; Li, S.; Wang, J.; Qi, D.; Lu, Q.; Xing, J. Distribution, occurrence mode, and extraction potential of critical elements in coal ashes of the Chongqing Power Plant. *J. Clean. Prod.* **2022**, *342*, 130910. [CrossRef]